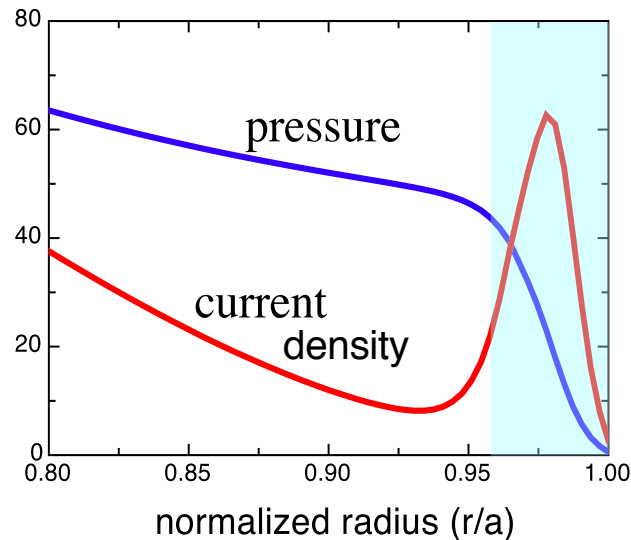


Summary

- ◆ The **edge current density $j(r)$** is measured to assess its influence on the stability and confinement in the **pedestal region**.
- ◆ Diagnostic Lithium beam, Zeeman effect are combined with a 32-channel polarimetry and spectroscopy system to determine local magnetic field profile.
- ◆ **Data from high δ , ELM-free H-mode experiment shows evidence for edge current peak. QH-mode also shows this peak.**
- ◆ **This presentation deals with using the measurements as constraints on equilibrium reconstructions for more accurate edge solutions. The stability of the resulting equilibria may then be assessed.**
- ◆ The current structure may also be calculated using Ampere's law and minimal information from equilibrium reconstruction.

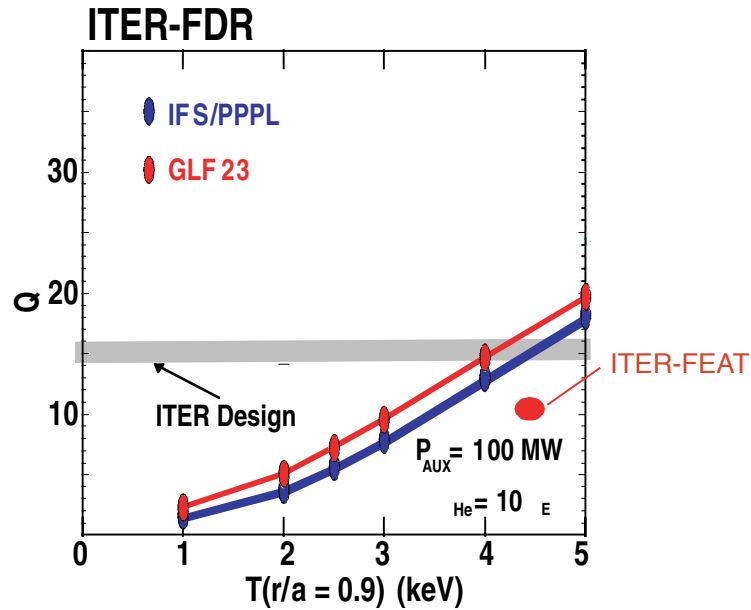
A successful ELM/ Pedestal model requires accurate knowledge of the local current density



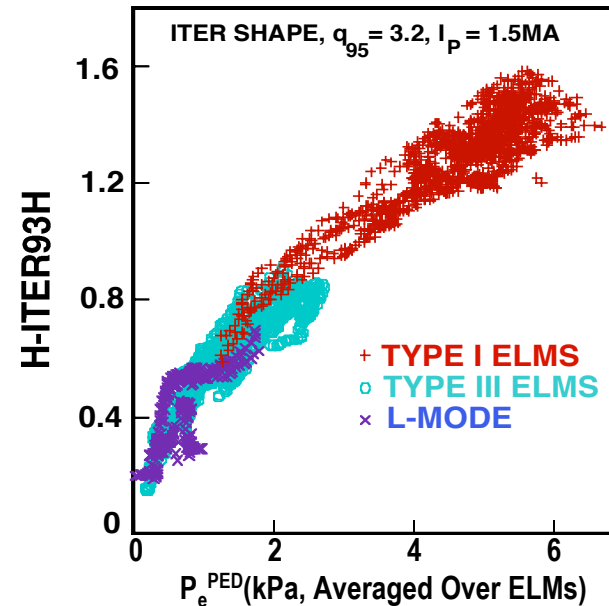
- ◆ Stability of the edge pressure pedestal is determined by a local current
- ◆ Current itself is driven by pressure gradient (bootstrap+P.S. current)
 - feedback driven limit on pedestal height
- ◆ We have evolved a successful ELM and pedestal model based on peeling-ballooning modes P. Snyder, 19thIAEA, 2001 APS
 - Quantitative pedestal stability limits and mode structures
 - Model has been verified against experiment
 - Predictive, if we knew the current distribution.

The Pedestal seems to be Key to Plasma Performance

- ◆ Both theory and experiment predict a strong dependence of core confinement, and therefore Q on the pedestal height (T_{ped}, p_{ped})



J.E. Kinsey, et al., *Berchtesgarten EPS*, III 1081 (1997)



T. Osborne, et. al., *Plas. Phys. and Contr. Fusion*

- ◆ ELM characteristics strongly impact divertor and wall heat load constraints (large Type I ELMs may not be tolerable in Burning Plasma devices)
- ➔ Goal is predictive understanding of physics controlling pedestal height and ELM characteristics \Rightarrow combination of high pedestal and tolerable ELMs

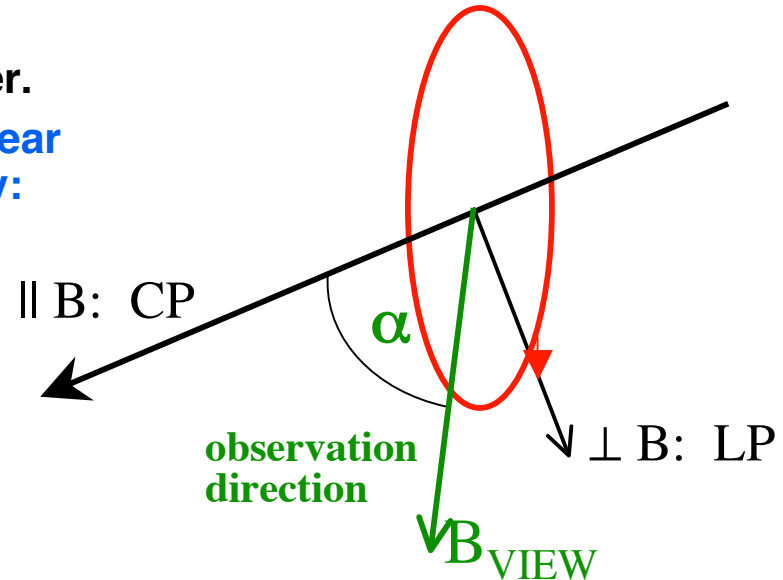
Lithium beam can be used to provide an accurate edge $j(r)$ determination

- ◆ **HOW:** Observe Zeeman components of the ${}^6\text{Li}$ 670.8 nm resonance line.
 - Quantum-mechanical effect, line has well determined splitting and polarization characteristics in a B field.
- ◆ Measurement is purely a B-field effect.
 - 2S-2P states ensures no Stark mixing
 - no electric field sensitivity/ambiguity
- ◆ Strategy: inject neutral lithium beam, analyze the polarization of emitted radiation in edge region, relate to B, infer $j(r)$.
- ◆ Small beam + large excitation rate = good signals, good spatial localization. Beam penetration sufficient for H-mode edges.

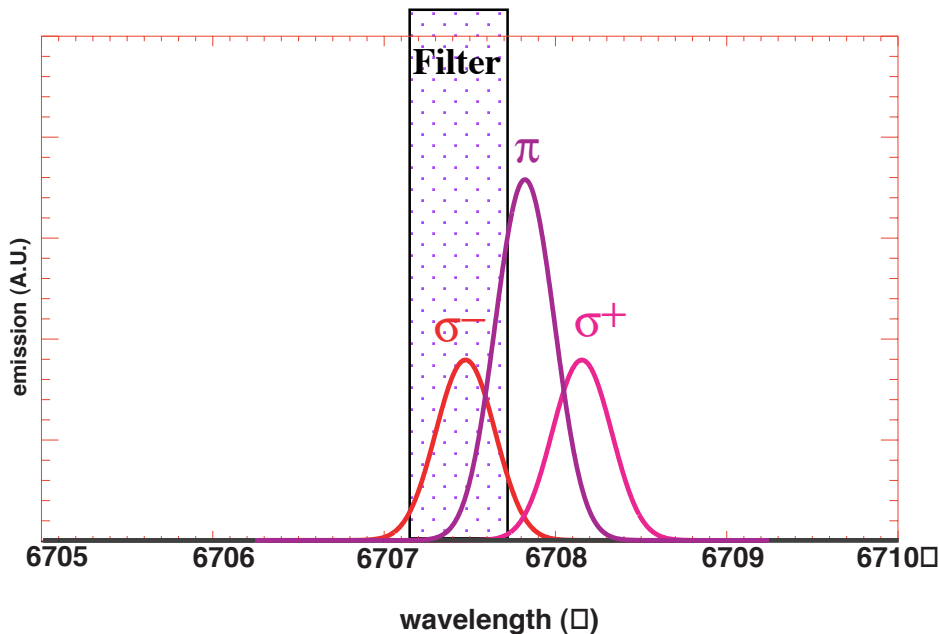
We determine the field direction by observing the σ Zeeman component of ${}^6\text{Li}$

- ◆ Select the σ - line with narrowband filter.
- ◆ Measure ratio of circular to linear polarization using dynamic polarimetry:

$$\text{Ratio} \left\{ \frac{\text{CP}}{\text{LP}} \right\} = \frac{2 \cos(\alpha)}{\sin^2(\alpha)}$$

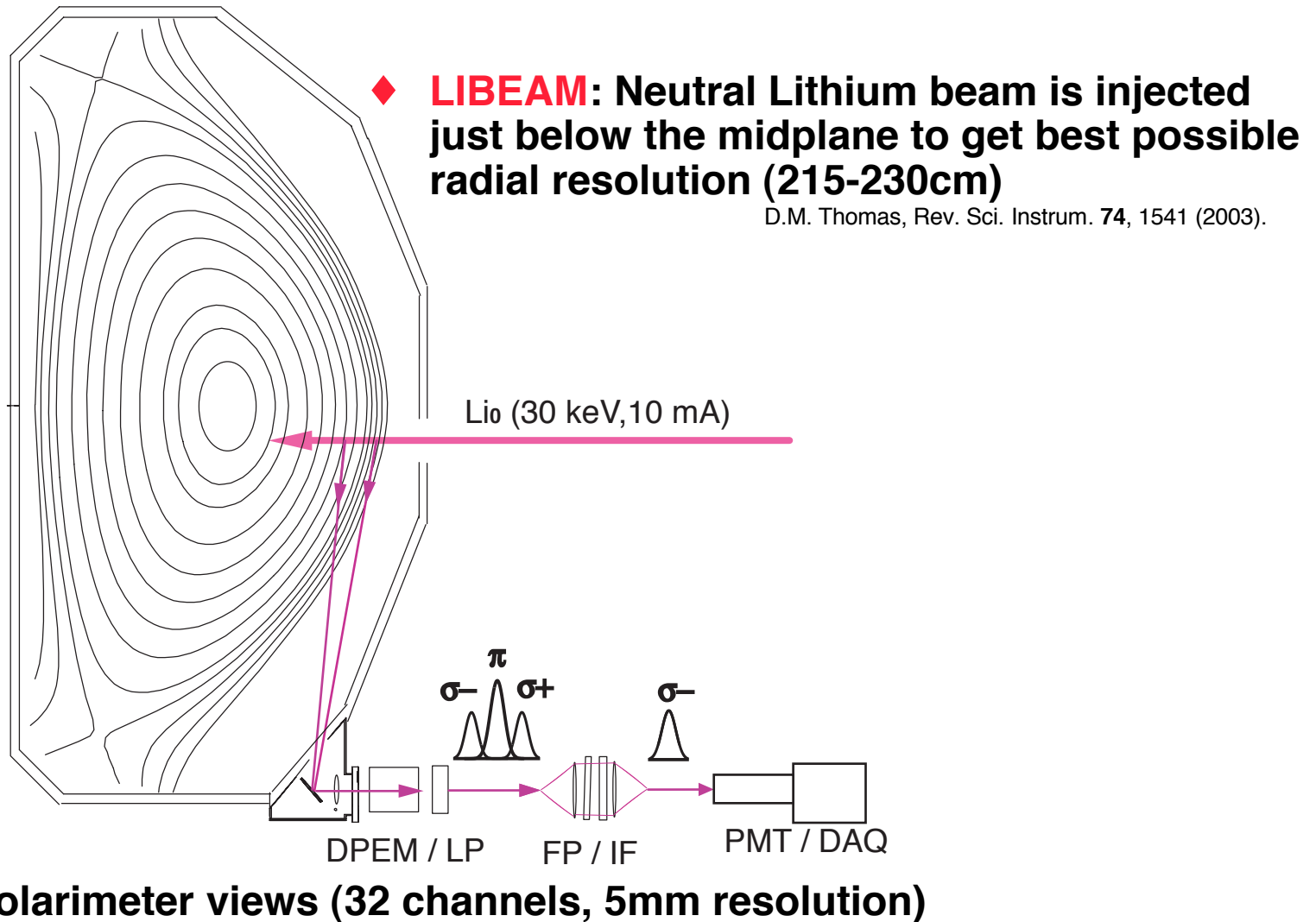


- ◆ Then $B_{\text{VIEW}}(R,z) = |B| \cos(\alpha)$
 - 1) use as EFIT constraint
 - 2) solve directly using



$$\mu_0 j_{\text{TOR}} = \frac{\partial B_R}{\partial z} - \frac{\partial B_z}{\partial R}$$

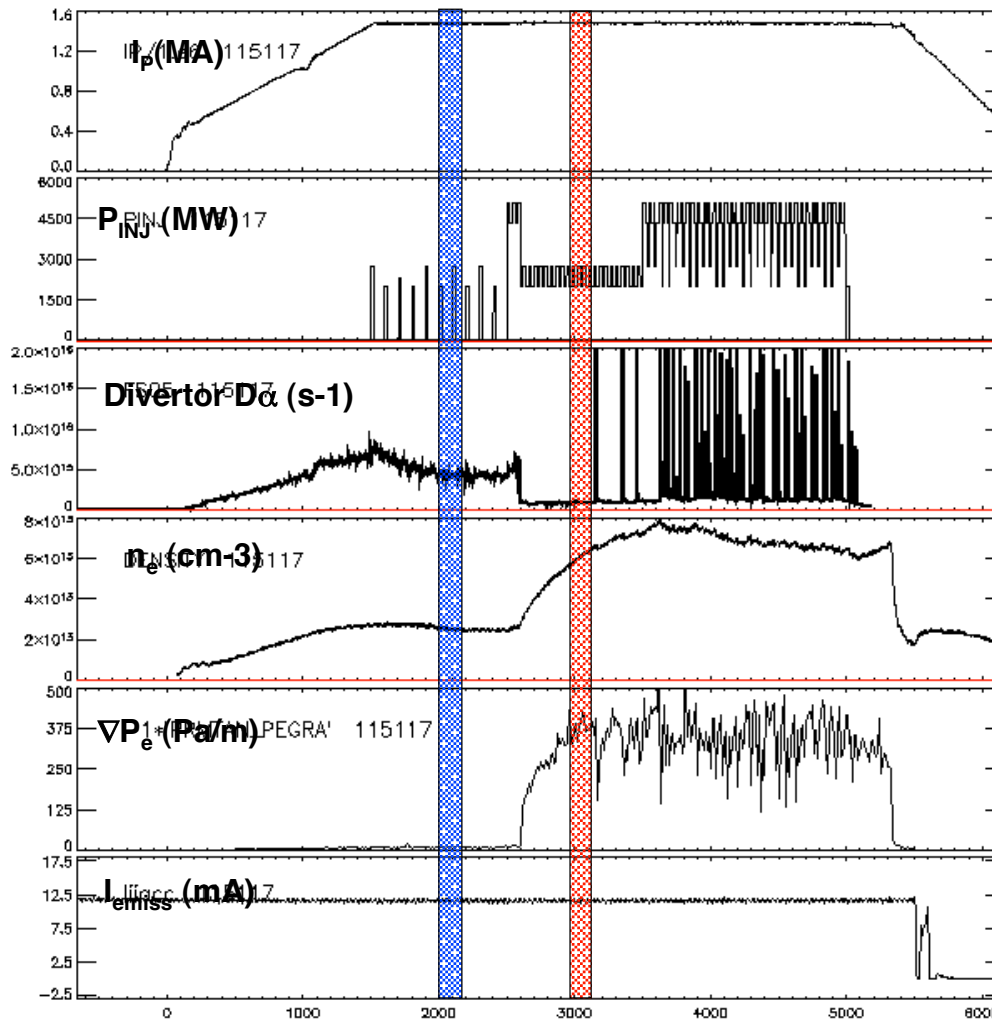
Installation on DIII-D Tokamak



Diagnostic Components

1. The 670 nm resonance fluorescence light from the collisionally excited beam is imaged at a series of closely spaced locations in the plasma edge.
2. The polarization state of the σ - Zeeman sublevel is analyzed by passing the light through dual photoelastic modulators (DPEM) and a linear polarizer (LP), which amplitude modulates the emission.
3. Signal is then passed through an individually tuned Fabry-Perot pair (FP) and an order blocking interference filter (IF) to isolate the σ - component for each of the Doppler-shifted viewing locations.
4. The filtered, amplitude modulated emission is then detected by GaAs photomultiplier tube (PMT) and digitized (DAQ).
5. Digital locking analysis at the first and second PEM harmonics recovers the circular and linear fraction of the σ - components. Their ratio determines the magnitude of $\cos(\alpha_{\text{VIEW}})$, where α_{VIEW} is the angle between the local magnetic field and each sightline.
6. Multiplication of $\cos(\alpha_{\text{VIEW}})$ by the total field yields B_{VIEW} , the component of magnetic field parallel to the sightline.

High Edge Pressure Gradient experiment



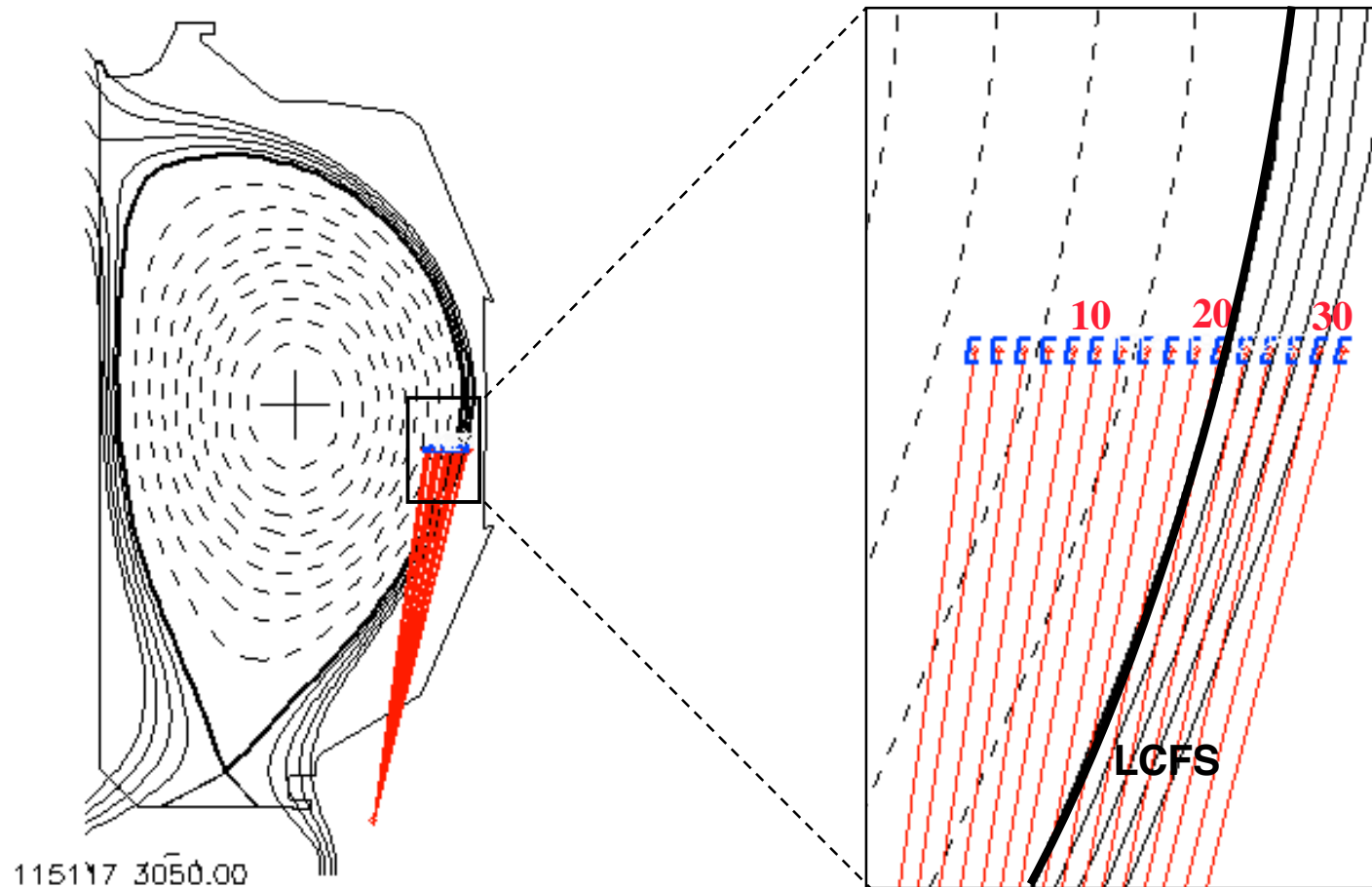
The L-H transition at 2600 ms is followed by an extended ELM-free period where the pedestal pressure rises to very high values. The pedestal pressure growth is then limited by intermittent giant Type 1 ELMS

LIBEAM is turned prior to shot to stabilize and is not modulated. Use companion shots for background assessment & correction

Compare measurements in **L-mode** (low pressure gradient), **ELM-free H-mode** (high pressure gradient)

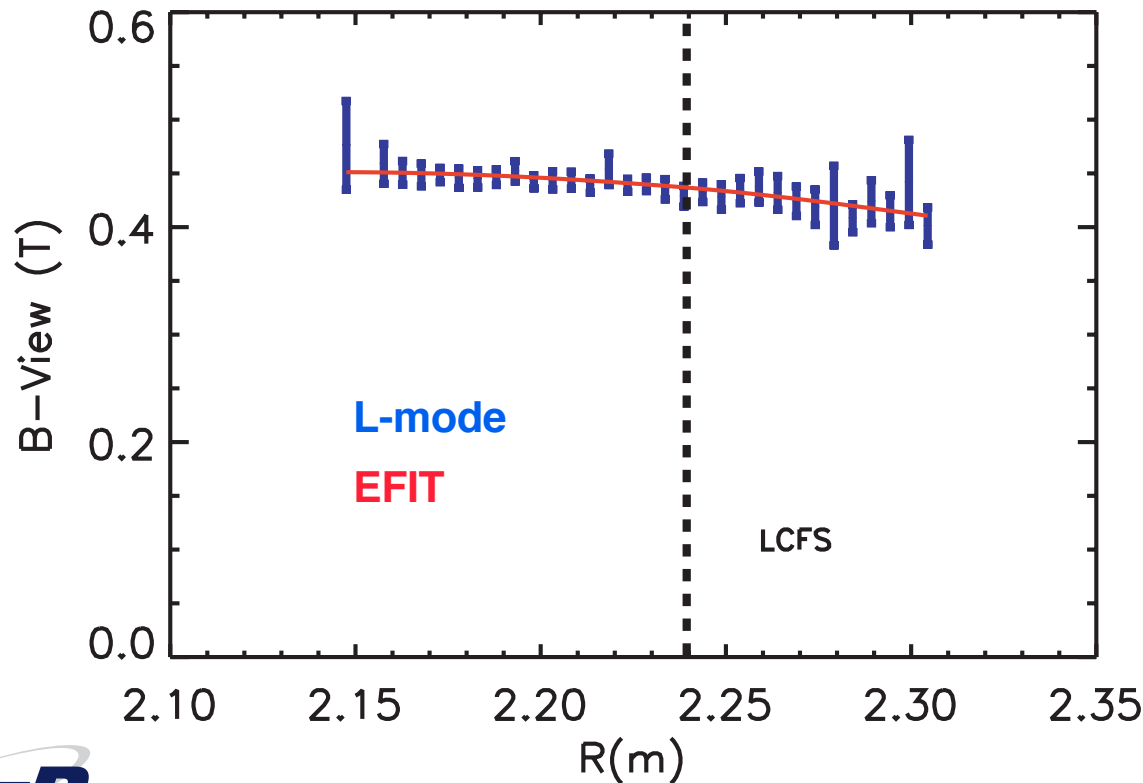
Viewchord array gives $d\psi_{\text{norm}} \sim 0.015$

- ◆ Good tangency to poloidal flux surfaces ($dR= 5\text{mm}$)
- ◆ Shot 115117-high δ , low n_e , long ELM-free H-mode phase



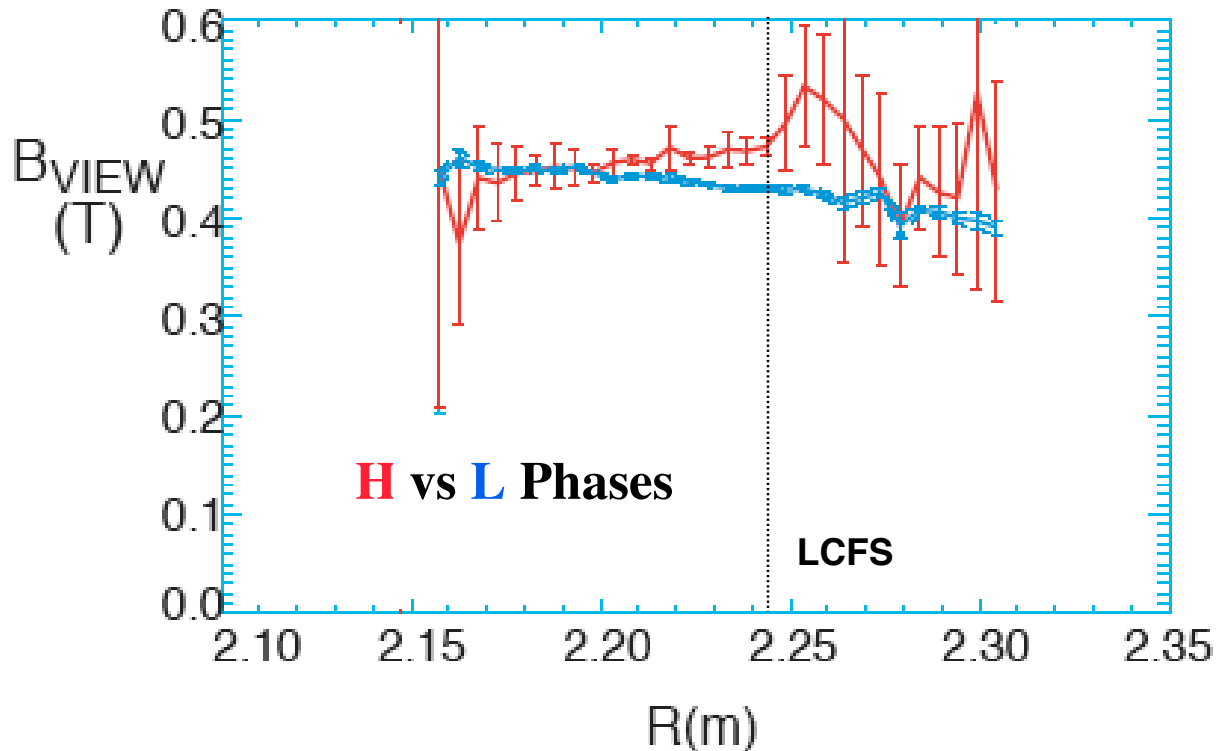
L-mode results (compared to EFIT)

- ◆ Field profiles are easily determined in L-mode
 - Small statistical error, due to low density, modest attenuation
 - Good data region covers most of edge.
 - Typically get very good agreement between the measured B_{VIEW} profile and that calculated from an EFIT reconstruction.(use ohmic calibration shot)
 - Very little structure seen in either data or EFIT (as expected)



H-mode Results (compared to L-Mode)

- ◆ Local magnetic field profile changes substantially during the ELM free H-mode phase
- ◆ Divergence in the two B_{VIEW} profiles near edge => **current peaking**

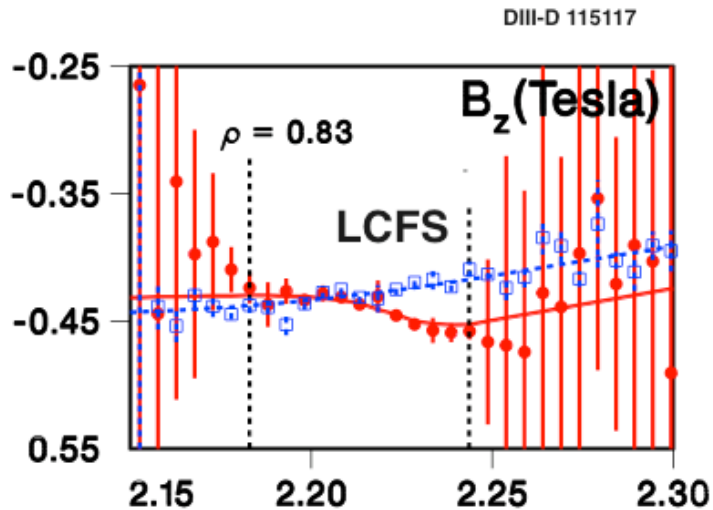


- Lower signal levels decrease time resolution - much noisier

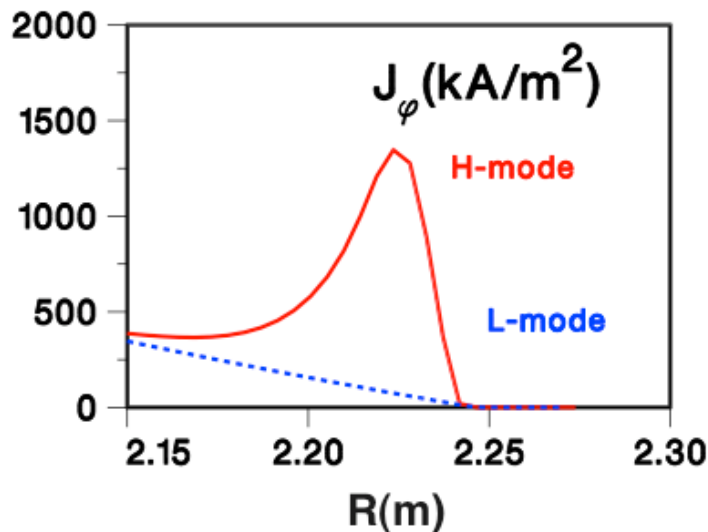
- Still have a 'sweet spot'- a range of R over which have small statistical errors

- A challenge to do direct comparison with EFIT, iterative solution required.

Inclusion of LIBEAM data in EFIT reconstructions: part 1

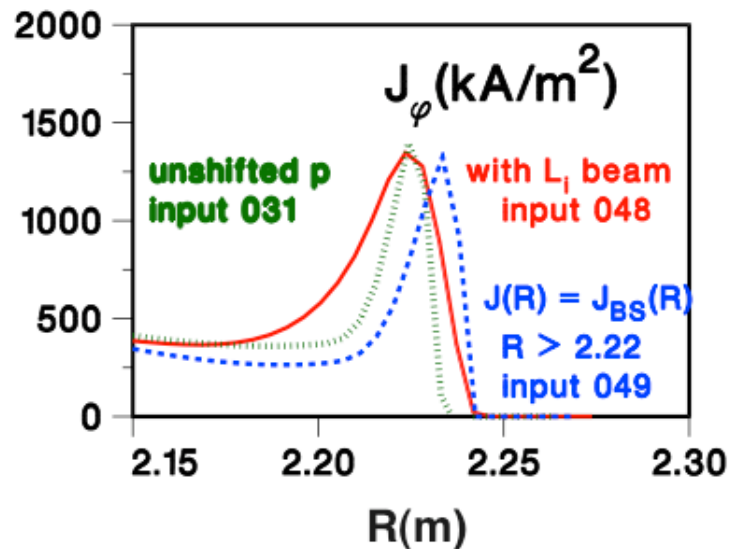
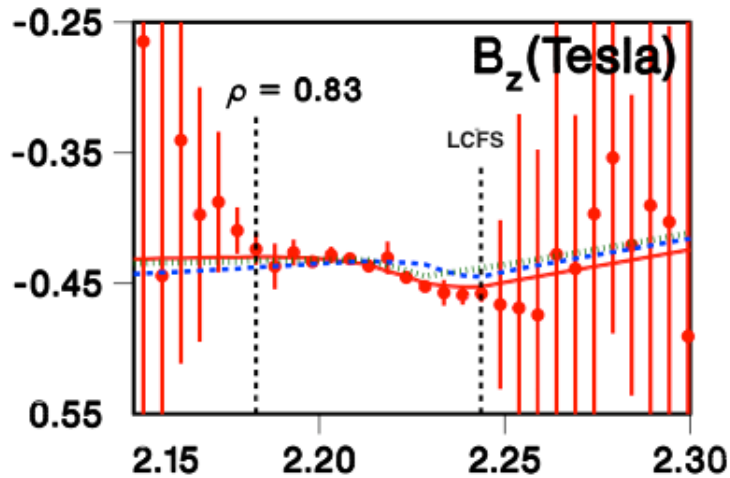


- ◆ The LIBEAM magnetic field profiles measured for shot 115117 during L- and H-mode are used as additional constraints on EFIT equilibrium solutions (including magnetics, MSE and the measured ion and electron pressure profiles). The resulting calculated B_z profiles from EFIT are plotted as solid (H) and dashed (L) lines.



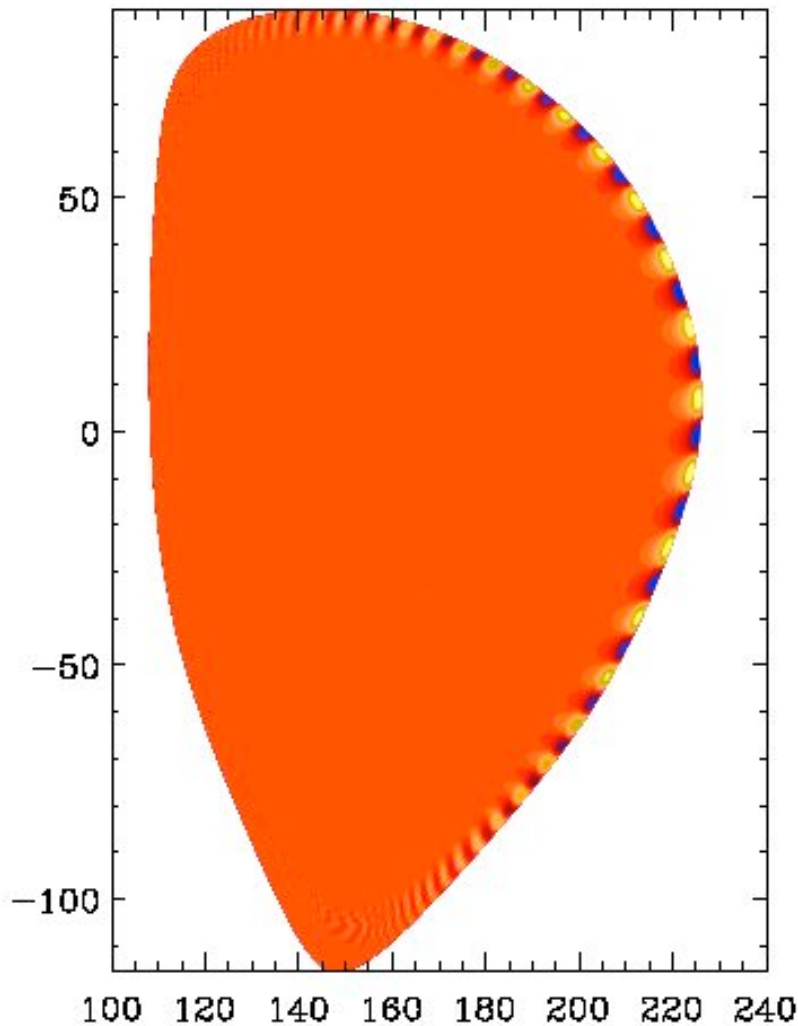
- ◆ The calculated toroidal current for the two cases are shown in the lower plot. The fit to the H-mode data shows a clear peak in the current density near the separatrix, with a peak value in excess of 1MA/m^2 .

Inclusion of LIBEAM data in EFIT reconstructions: part 2



- ◆ Next we compare the current density indicated by the lithium beam measurement with the calculated bootstrap current in the H-mode case.
- ◆ The calculated toroidal current is shown in red. The two dashed curves (blue and green) are from two different equilibrium reconstructions using the measured pressure profiles and a current density near the edge which is constrained by a bootstrap current calculated using the NCLASS model. The two curves represent slightly different boundary conditions on the pressure profile parameterization within the EFIT grid.

Stability Calculations



- ◆ Preliminary ELITE runs using the equilibria above indicate stability for the low-n modes ($n < 15$), marginal stability for modes of medium n (20-25) and instability for modes having $n = 30-35$.
- ◆ This is consistent with the approach to ELM onset expected from the stability model, where lower and lower n modes become successively unstable.
- ◆ Shown is the mode structure for $n=25$, indicating the approximate depth of the perturbation.

(also see [Snyder, P2-156](#), this session)

Ampere's Law approach-1

- ◆ Because of the extreme sensitivity of the equilibria to the highly localized details of the current density, an iterative approach must be taken to obtain the most accurate solutions prior to performing the stability tests. This is painful and has prevented large scale, systematic scans of various parameters to assess the empirical scaling of stability with edge current for differing collisionalities, pedestal scale lengths, etc.
- ◆ **An alternative approach is to use Ampere's law to interpret Lithium beam data directly, using known spatial calibration, estimate of field inclination in region of interest (from EFIT).**
 - Similar technique used by Petty et al. for central ECCD MSE interpretation (NF,2000)
- ◆ This allows us to derive a straightforward parameterization for $J_{\text{TOR}}(r)$ in terms of B_{VIEW} , $d(B_{\text{VIEW}})/dR$, $\tan\theta_B$ and its derivatives.
- ◆ Derivative error on measurement is main uncertainty in this approach.

Ampere's Law approach-2

- ◆ The spatial calibration defines the R, z location for each of the viewchords (red lines) as well as the view inclination angle θ_V -

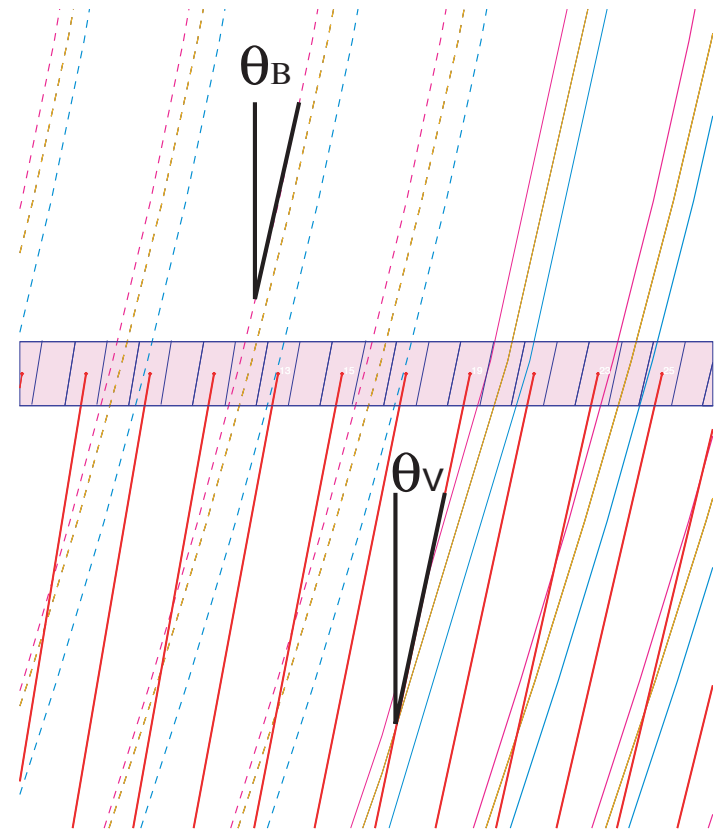
$$B_{VIEW} = B_Z \cos\theta_V + B_R \sin\theta_V$$

- ◆ Or, using the magnetic inclination angle θ_B ($\tan\theta_B = B_R/B_Z$)

$$B_{VIEW} = B_Z (\cos\theta_V + \sin\theta_V \tan\theta_B)$$

- ◆ **ADVANTAGE:** $\tan\theta_B$ is an insensitive function of the exact current distribution

⇒ can evaluate using any reasonable reconstruction (dotted lines).



Ampere's Law approach-3

Then Ampere's law

$$\mu_0 j_{TOR} = \frac{\partial B_R}{\partial z} - \frac{\partial B_z}{\partial R}$$

may be written

$$\mu_0 j_{TOR} = \frac{\partial B_z}{\partial z} \tan \theta_B + B_z \frac{\partial \tan \theta_B}{\partial z} - \frac{\partial B_z}{\partial R}$$

and, from the definition of poloidal flux function in toroidal geometry

$$B_R = -\frac{1}{R} \frac{\partial \varphi}{\partial z}, \quad B_z = \frac{1}{R} \frac{\partial \varphi}{\partial R}$$

we can take the appropriate partials to get

$$\frac{\partial B_z}{\partial z} = -\frac{1}{R} \frac{\partial}{\partial R} (R B_R) = -\frac{B_R}{R} - \frac{\partial B_R}{\partial R}$$

Ampere's Law approach-4

Or, again using the definition of $\tan\theta_B$

$$\frac{\partial B_z}{\partial z} = -B_z \frac{\tan\theta_B}{R} - \frac{\partial B_z}{\partial R} \tan\theta_B - B_z \frac{\partial \tan\theta_B}{\partial R}$$

And Ampere's law may be written

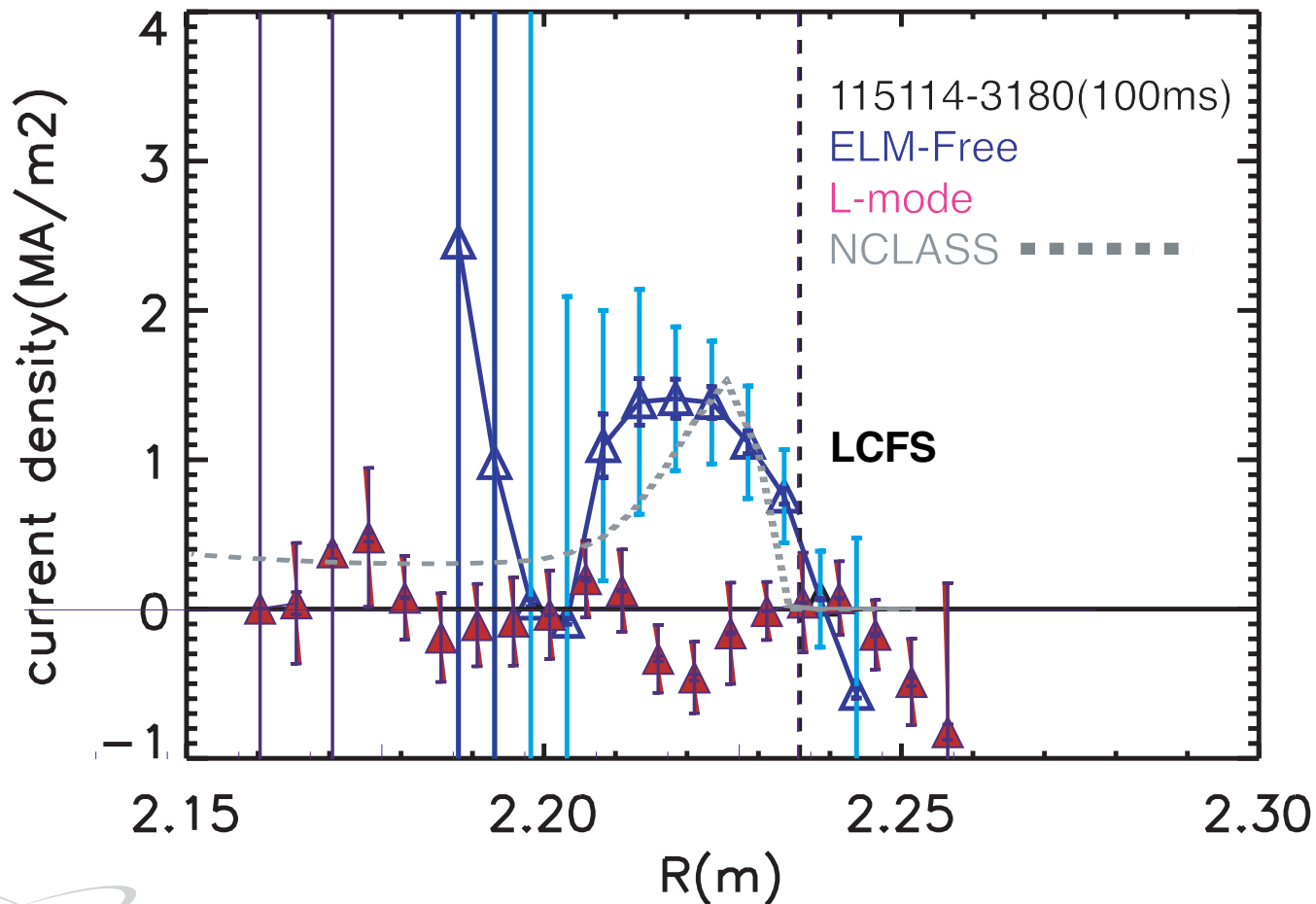
$$\mu_0 j_{TOR} = B_z \left(\frac{\partial \tan\theta_B}{\partial z} - \frac{\tan^2\theta_B}{R} - \tan\theta_B \frac{\partial \tan\theta_B}{\partial R} \right) - \frac{\partial B_z}{\partial R} (1 + \tan^2\theta_B)$$

Finally, substituting for B_z with B_{VIEW} yields

$$\begin{aligned} \mu_0 j_{TOR} = & B_{VIEW} \frac{\left[\frac{\partial \cos\theta_V}{\partial R} + \frac{\partial \sin\theta_V}{\partial R} \tan\theta_B + \sin\theta_V \frac{\partial \tan\theta_B}{\partial R} \right] [1 + \tan^2\theta_B]}{\left[\cos\theta_V + \sin\theta_V (\tan\theta_B) \right]^2} \\ & + B_{VIEW} \frac{\left[\frac{\partial \tan\theta_B}{\partial z} - \frac{\tan^2\theta_B}{R} - \tan\theta_B \frac{\partial \tan\theta_B}{\partial R} \right]}{\left[\cos\theta_V + \sin\theta_V (\tan\theta_B) \right]} - \frac{\partial B_{VIEW}}{\partial R} \left[\frac{1 + \tan^2\theta_B}{\cos\theta_V + \sin\theta_V (\tan\theta_B)} \right] \end{aligned}$$

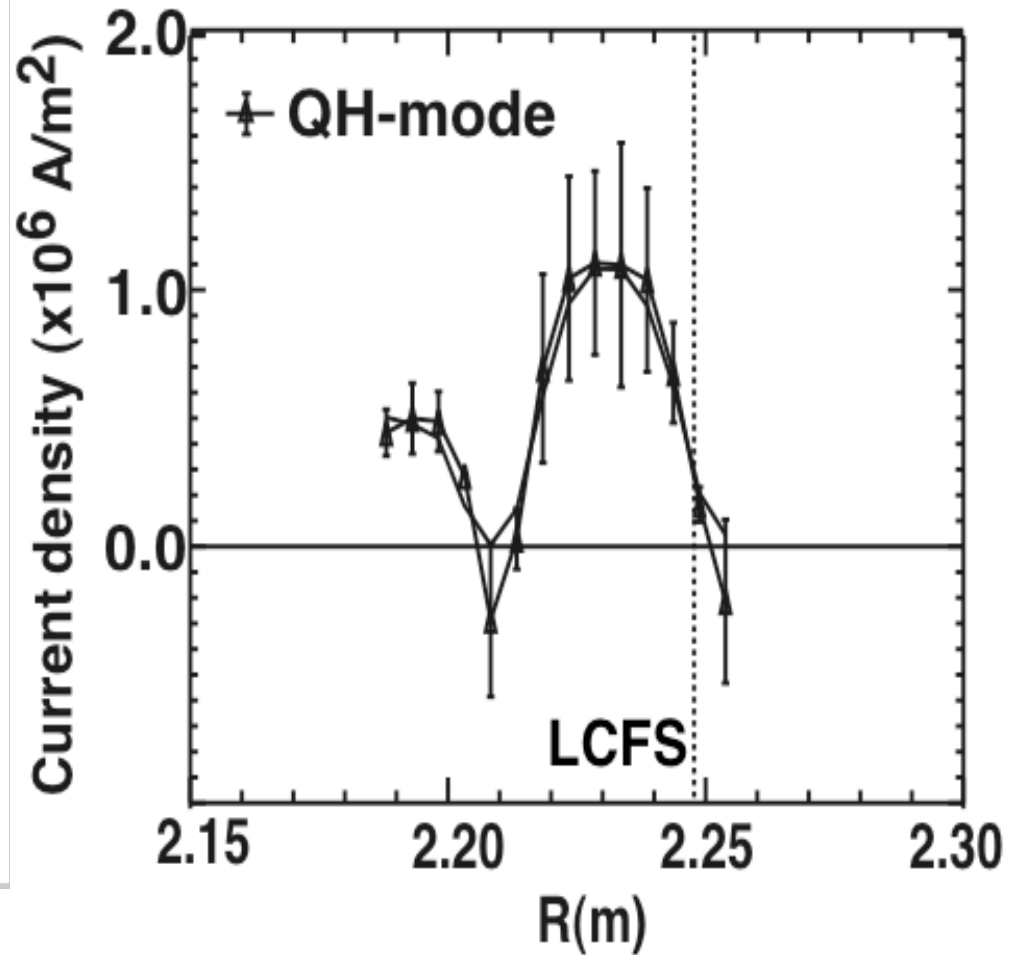
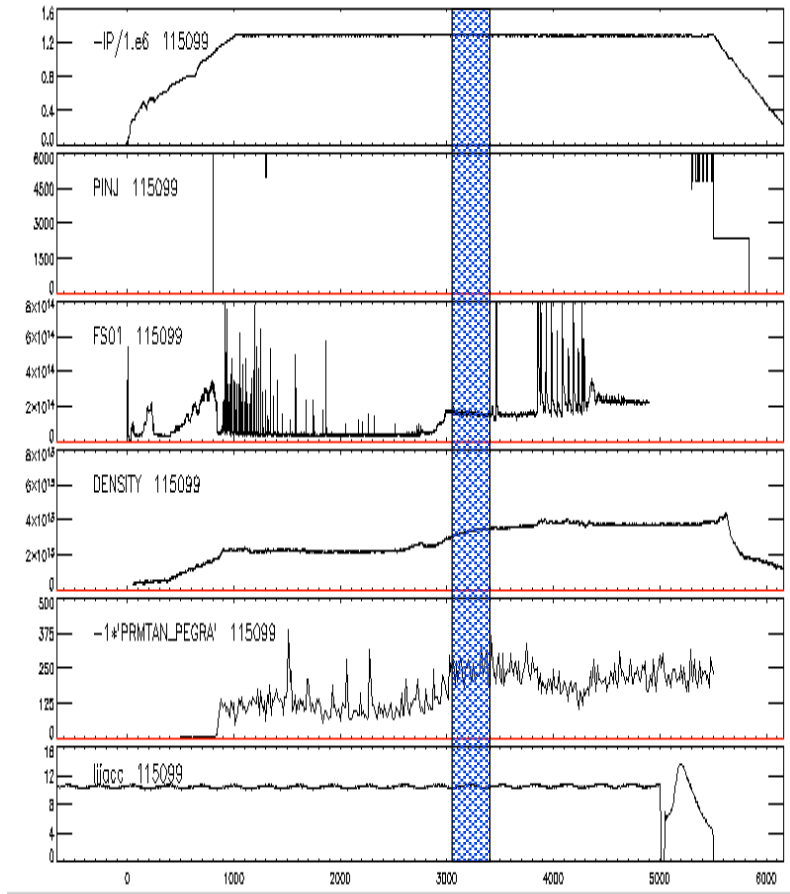
J_{TOR} : Initial comparison with model

- ◆ Comparison with Kinetic EFIT prediction based on measured pressure profiles
- ◆ EFIT current shape constrained by NCLASS bootstrap model in edge
- ◆ Rough qualitative agreement



QH-mode Results

Find somewhat lower current peak (lower ∇p)



Conclusions

- ◆ On DIII-D, for cases where there is an appreciable edge pedestal and associated pressure gradient, using the LIBEAM diagnostic we find large localized currents in the region of the gradient, near the last closed flux surface.
 - ELM-free H-mode-see evidence for 1-2 MA/m² at time of peak ∇p .
 - Elming phase is somewhat lower.
 - QH-mode also somewhat lower.
 - L-mode---no discernible current or structure.
- ◆ The measured poloidal field profile has been used in EFIT reconstructions. ELITE stability calculations using the resulting equilibria indicate modes in the range $n=20-25$ are marginally stable shortly before the first ELM crash. The reconstructions are sensitively dependent on the details of the profile and require an iterative approach to get the most accurate reconstruction and stability assessment.
- ◆ Using Ampere's Law and minimal information from EFIT, we can interpret the measurements to estimate J_{TOR} directly, without recourse to a detailed reconstruction. The amplitude is consistent with the measured pressure profile and a collisional bootstrap current.